České vysoké učení technické v Praze
Fakulta jaderná a fyzikálně inženýrská

Czech Technical University in Prague
Faculty of Nuclear Sciences and Physical Engineering

Doc. Dr. RNDr. Miroslav Karlík

STUDIUM GUINIER-PRESTONOVÝCH ZÓN VE SLITINÁCH NA BÁZI Al-Cu V ATOMOVÉM ROZLIŠENÍ

ATOMIC RESOLUTION INVESTIGATION OF GUINIER-PRESTON ZONES IN Al-Cu BASED ALLOYS

Summary

Precipitation hardening was discovered by Wilm in 1906 during the study of the influence of Mn addition on the Al–Cu–Mg alloy. After rapid cooling, the material spontaneously hardened during the period of four days. Already in 1908 the alloy, with the composition of (wt%) 3–4.5% Cu, 0.4–1.0% Mg, and 0.2–0.7% Mn, has been patented and commercialized under the name of DURALUMIN.

The cause of the hardening remained unknown till 1919 when Merica suggested that it is due to the formation of sub-microscopic particles. The structure of these particles, so called Guinier-Preston (GP) zones, was first described in 1938 independently by Guinier and Preston, who studied binary Al–Cu alloys by means of different techniques of X-ray diffraction.

The first micrographs of GP zones recorded in the diffraction contrast in the transmission electron microscope were published at the end of fifties by Nicholson and Nutting. The dream of the researchers – to be able to study the structure of the GP zones in an atomic resolution – started to be realized in the seventies, when Phillips visualised the fringes of (100) atomic planes in the Al–Cu alloy. The first generation of the microscopes with resolution of 0.19 nm, constructed in the nineties, enabled the study of the GP zones in an atomic resolution.

This lecture summarizes the results of the investigation of the structure and Cu content of Guinier-Preston zones in three Al–Cu based alloys – an industrial 2017A alloy Al–3.69Cu–0.96Mg–0.65Mn wt% and two binary alloys containing 4.22 wt% (1.84 at%) and 3.41 wt% (1.54 at% Cu), respectively – by means of complementary techniques of high resolution electron microscopy (HREM), field ion microscopy (FIM) and tomographic atom probe (TAP).

The HREM experimental images are interpreted using multislice simulations. The majority of GP1 zones in the Al–4.22 wt% Cu alloy consist of atomic monolayers, the disc diameter ranging from 4 to 10 nm. The contrast of the GP1 zones is strongly dependent on their size, on the foil thickness, on the defocus of the objective lens, less sensitive to the Cu content and much less sensitive on the position of the GP zone in the depth of the foil.

Results on Guinier-Preston zones in a monocrystal of the Al–3.41 wt% Cu alloy annealed for 30 h at 100°C confirm that majority of GP1 zones are monolayers 1 to 9 nm in size. However, some GP2 zones and particles in an intermediate state of growth between GP1 and GP2 stage were also found.

From TAP results in the Al–3.41 wt% Cu alloy it follows that GP1 zones with different Cu concentrations ranging from 40% up to 100% Cu coexist. The residual solid solution is very heterogeneous. In the vicinity of GP particles the Cu content in the matrix falls down to zero, the solid solution in other regions contains from 1.6 to 2.3 wt% Cu (0.7 to 1 at% Cu).

Souhrn

Precipitační zpevnění bylo objeveno Wilmem v roce 1906 během studia vlivu Mn na slitinu Al–Cu–Mg. Po zakalení slitiny bylo pozorováno spontánní zvyšování tvrdosti materiálu po dobu 4 dnů. Studovaná slitina, se složením (hm%) 3–4,5% Cu, 0,4–1,0% Mg a 0,2–0,7% Mn byla již v roce 1908 patentována a vyráběna pod obchodní značkou DURALUMIN.

Příčina zpevnění zůstala neznámá až do roku 1919, kdy Merica navrhl, že je způsobena submikroskopickými částicemi. Struktura těchto částic, tzv. Guinier-Prestonových (GP) zón, byla poprvé popsána v roce 1938 Guinierem a Prestonem, kteří nezávisle na sobě studovali binární slitinu Al–Cu různými metodami difrakce rentgenového záření.

První snímky GP zón v difrakčním kontrastu pořízené pomocí transmisního elektronového mikroskopu byly publikovány na konci padesátých let Nicholsonem a Nuttingem. Sen vědeckých pracovníků – moci pozorovat strukturu GP zón v atomovém rozlišení – se začal realizovat v sedmdesátých letech, kdy Phillips zviditelnil proužky atomových rovin (100) slitiny Al–Cu. V devadesátých letech byla vyrobena první generace mikroskopů s rozlišovací schopností 0,19 nm, které umožnily studium GP zón v atomovém rozlišení.

Tato přednáška shrnuje výsledky studia struktury a obsahu Cu v Guinier-Prestonových (GP) zónách ve třech materiálech na bázi Al–Cu: průmyslové slitině 2017A se složením Al–3,69Cu–0,96Mg–0,65Mn hm% a dvou modelových binárních slitinách obsahujících 4,22 hm% (1,84 at%) a 3,41 hm% (1,54 at%) Cu. Ke studiu byly použity komplementární experimentální techniky: transmisní elektronová mikroskopie s atomovým rozlišením (high resolution electron microscopy - HREM), iontová mikroskopie (field ion microscopy - FIM) a tomografická atomová sonda (tomographic atom probe - TAP).

Snímky z elektronového mikroskopu jsou interpretovány pomocí počítačových simulací metodou multivrstev. Většina GP1 zón ve slitině Al–4,22 hm% Cu má tloušťku jediné atomové vrstvy, o velikosti disku v rozmezí 4 až 10 nm. Kontrast GP zón je silně závislý na jejich velikosti, rozostření čočky objektivu a tloušťce tenké fólie.

Výsledky studia GP zón v monokrystalu slitiny Al–3,41 hm% Cu stárnuté 30 h při 100 °C potvrdily předchozí zjištění, že většina GP1 zón má tloušťku jediné atomové vrstvy a průměr částic se pohybuje v rozmezí 1 až 9 nm. Avšak byly pozorovány i částice GP2 nebo částice v intermediálním stádiu růstu od fáze GP1 ke struktuře GP2.

Z chemické analýzy v atomovém rozlišení pomocí tomografické atomové sondy vyplývá, že ve slitině s obsahem 3,41 hm% Cu koexistují částice GP1 zón obsahující 40 až 100% Cu. Reziduální tuhý roztok je velmi heterogenní. V blízkosti GP zón jeho koncentrace klesá až k nule, průměrná koncentrace v ostatních částech matrice se pohybuje v rozmezí 1,6 až 2,3 hm% Cu (0,7 až 1 at% Cu).

Klíčová slova
Slitiny hliníku; Fázové transformace; Transmisní elektronová mikroskopie s atomovým rozlišením; Iontová mikroskopie; Tomografická atomová sonda

Keywords
Aluminium alloys; Phase transformations; High-resolution electron microscopy; Field ion microscopy; Tomographic atom probe

---

České vysoké učení technické v Praze
Název: Studium Guinier-Prestonových zón ve slitinách na bázi Al-Cu v atomovém rozlišení
Autor: Doc. Dr. RNDr. Miroslav Karlík
Počet stran: 35
Náklad: 150 výtisků

ISBN

CONTENTS

1. INTRODUCTION

An important metallurgical problem which still has not been solved completely is the question how phase separation is initiated and progresses during the early stages of solid solution decomposition when large parts of the sample are still in a supersaturated state. In many alloys, e.g. Al-Zn, Cu-Be, Fe-Mo, Al-Ag, Al-Cu or Al-Mg-Si, the decomposition (and hardening) process starts by forming small clusters of solute atoms – Guinier-Preston (GP1) zones. Their morphology (platelets, spheres, needles) depends on the interfacial energy and coherency strain energy. The decomposition of the supersaturated solid solution (SSS) in the Al–Cu system shows a variety of metastable states, following the sequence:

$$\text{SSS} \rightarrow \text{GP1 zones} \rightarrow \text{GP2 zones } (\theta'') \rightarrow \theta' \rightarrow \theta \ (\text{CuAl}_2).$$

GP1 and GP2 zones are pre-precipitates coherent with the matrix, the intermediate precipitate θ' is semi-coherent and the equilibrium precipitate θ is incoherent. The first evidence of the pre-precipitate particles was found in Al-Cu alloys in late thirties independently by Guinier [1] and Preston [2] who applied different X-ray techniques. In their original models, Guinier and Preston described GP (GP1) zones as Cu-rich thin platelets coherent on the {100} Al matrix planes. In the fifties, again using X-rays, Guinier [3] identified the θ'' phase (later designed GP2) as two Cu-rich layers separated by three atomic layers of the Al matrix. Since the seventies, the structure of both these phases was confirmed by other authors using computer analysed diffuse X-ray scattering [4,5], field ion microscopy (FIM) [6–9] or in transmission electron microscopy (TEM) in different high-resolution electron microscopy (HREM) modes [10–12]. It has also been found that the GP1 zone variants composed of two or more layers of Cu atoms coexist with the monolayer zones. Nevertheless, the volume fraction of these multilayer zones remains still under question, ranging from 13% [13] to 25% [4,5].

If there is a general agreement on the morphology of the GP1 zones (platelets, the majority of them being monolayers), their Cu content and the adjacent strain field are still points of controversy. According to recent results, the displacement of first neighbouring matrix planes ranges from 3.2% [14] to 17 % of the {200} interplanar spacing of Al matrix [5, 15,16].

As for the Cu content, Auvray *et al.* [4], Matsubara and Cohen [5], Gerold and Bubeck [17] reported 100% Cu in the GP1 zones. On the other hand, Fontaine *et al.* [15] proposed a model of 50%Cu / 50% Al. An atom probe analysis (Al-1.7 at% Cu alloy aged 130 °C/ 16.7 h) by Hono *et al.* [8, 18] gave the Cu content of Cu rich planes to be even smaller, between 25 and 45 %. As for the depleted matrix (Cu solid solution), a Cu content of 0.75 at% has been found. This is in a good agreement with the value of 1 at% obtained in Al–2.0at%Cu and Al–2.5at%Cu alloys aged 90 °C/ 50 h and 240 °C/ 50 h by

Fontaine *et al.* [15] using extended X-ray absorption fine structure (EXAFS) technique. On the other hand, Auvray *et al.* [4] claimed that there was no significant Cu content in the matrix. Using wide-angle and small-angle scattering of X-rays and neutrons, Malik *et al.* [19] found recently that 90 % of GP1 zones are monolayers, composed of 84 ± 2 at% Cu, while the Cu fraction in the matrix is 0.35 at%. For a more detailed review of these controversial results see the *Scripta Metallurgica* Viewpoint Set edited by Gerold [20] or Al–Cu parts of review papers by Schönfeld [21] or Ringer and Hono [22]. Lately, GP zones were investigated by high-angle annular dark field imaging in scanning transmission electron microscopy by Konno *et al.* [23]. The recently developed tomographic atom probe (TAP) [24] has a potential to carry out an atom-by-atom three dimensional (3D) compositional analysis of the GP1 zones and of the surrounding solid solution and so to bring new results.

This lecture summarizes the results of an atomic resolution investigation of Guinier-Preston zones in Al–Cu based alloys alloy using HREM lattice imaging interpreted by multislice simulation calculations of the contrast of the experimental images [25,26], in combination with field-ion microscopy (FIM) and 3D compositional analysis by means of the tomographic atom probe (TAP) [27].

2. EXPERIMENTAL DETAILS

Three Al–Cu based alloys were investigated: an industrial 2017A alloy Al–1.68Cu–1.10Mg–0.33Mn at% (Al–3.69Cu–0.96Mg–0.65Mn wt%), and two binary alloys containing 1.84 at% (4.22 wt%) Cu and 1.54 at% (3.41 wt%) Cu, respectively.

The 2017A type industrial alloy was supplied in the form of a sheet 1.5 mm thick in the T3 temper (solution annealed at 495 °C, quenched, pre-strained 2% and naturally aged for more than 2 years). The binary alloys were prepared in the laboratory from high purity metals (Al 5N, Cu 4N5). A strip of the Al–1.84 at% Cu alloy was cold rolled to 0.15 mm, solution annealed at 540 °C for one hour, quenched into ice water and aged 10 hours at 100 °C. A single crystal of the Al–1.54 at% Cu alloy, 80 mm long and 6 mm in diameter, prepared by the Bridgman method was homogenized at 530°C for one week, solution annealed at 540°C for 4 hours and, after quenching in ice water, aged for 30 hours at 100°C. It was then oriented by X-ray diffraction in order to cut, with a slow speed diamond saw, slices 0.30 mm in thickness, parallel to the {110} crystal planes.

Standard TEM specimen preparation procedure (diamond disc cutting, punching, mechanical polishing and electrolytic twin-jet polishing) was employed to obtain thin foils 3 mm in diameter. The electrolytic twin-jet polishing was carried out in the TENUPOL 2 (Struers) apparatus filled by the electrolyte composed of 30 ml of nitric acid dissolved in the solution of 300 g copper nitrate in 900 g of methanol. The approximate conditions of polishing were T = –10 °C, U = 25 V and I = 190 mA. Methanol was used to rinse the foils.

High resolution electron microscopy observations were carried out at 200 kV with the Philips CM20 instrument at École Centrale Paris, equipped with an UltraTwin objective lens (C_S = 0.5 mm), a LaB_6 gun and a CCD camera. The atomic resolution micrographs were taken in both possible crystallographic orientations, [100] and [110], under symmetric (axial) illumination conditions.

The experimental images were interpreted using the EMS software [28]. According to the experimental conditions, the following parameters were used to calculate the simulations: objective aperture diameter = 23 nm^{-1} (21 and 23 beams in the <100> and <110> zone axis respectively), defocus spread = 10 nm, semi-angle of convergence of the incident beam = 1 mrad, Debye-Waller parameter = 0.005. The images were calculated without absorption, with the resolution 0.5×10^{-2} nm, suggested by the EMS program; it means in the sampling 512 × 512 incident beams for used super-cells.

From the oriented slices, small rods 0.3 mm × 0.3 mm × 20 mm in dimensions oriented parallel to the <100> crystal direction, were cut by low-speed diamond sawing. Very sharp needle-shaped specimen for TAP-FIM were electropolished in a solution of 33% HNO3 in methanol cooled to –10°C, at 5 to 8 V DC.

Field-ion microscopy (FIM) observations and chemical analyses were performed with the tomographic atom probe (TAP) designed at Rouen University. This instrument can be used either as a projection microscope, based on the field ionisation of a rare gas near the surface of the sample, or as a three dimensional atom probe, in which the material is field evaporated by high voltage pulses. In this analysis mode, the TAP is an ultra-high vacuum instrument equipped with a time of flight mass spectrometer and a detector sensitive to the position of ion impacts [24]. The analysed volume of material is *a posteriori* reconstructed in three dimensions on a sub-nanometric scale. A few 100 000 ions are collected per analysis. The corresponding dimensions of the analysed volume are usually 10 nm × 10 nm × 50 nm.

The best imaging conditions for aluminium base alloys were obtained under 2×10^{-3} Pa of helium, with a sample temperature of 15 K. Analyses were carried out along the $<001>_{Al}$ direction, in an ultra-high vacuum better than 10^{-8} Pa, with a tip temperature of 30 to 35 K, a DC voltage of 4 to 10kV and a pulse to DC voltage ratio of 19 %. Mass spectra show the following features: copper field-evaporates as singly charged ions and aluminium as singly and doubly charged ions. Some Al and Cu atoms were also detected as AlH^+, AlH_2^+, AlH_3^+ and CuH^+, CuH_2^+ hydrides. They were taken into account in composition calculations. The average composition of the alloy, obtained from all data collected during TAP analyses (3.66×10^6 ions) is 1.54 ± 0.01 at% Cu. This is in a very good agreement with the global chemical analysis.

3. RESULTS AND DISCUSSION

3.1. HREM contrast of GP zones

A general micrograph of GP1 zones in Al–1.68Cu–1.10Mg–0.33Mn at% alloy (2017A – T3) in the <100> zone axis orientation of the crystal is shown in Fig. 1. In this orientation, (200) and (020) planes of the crystal are visualised. Their interplanar spacing, 0.202 nm, is close to the limit of the resolution of the microscope (0.19 nm) and thus the contrast is not so strong, but rather damped.

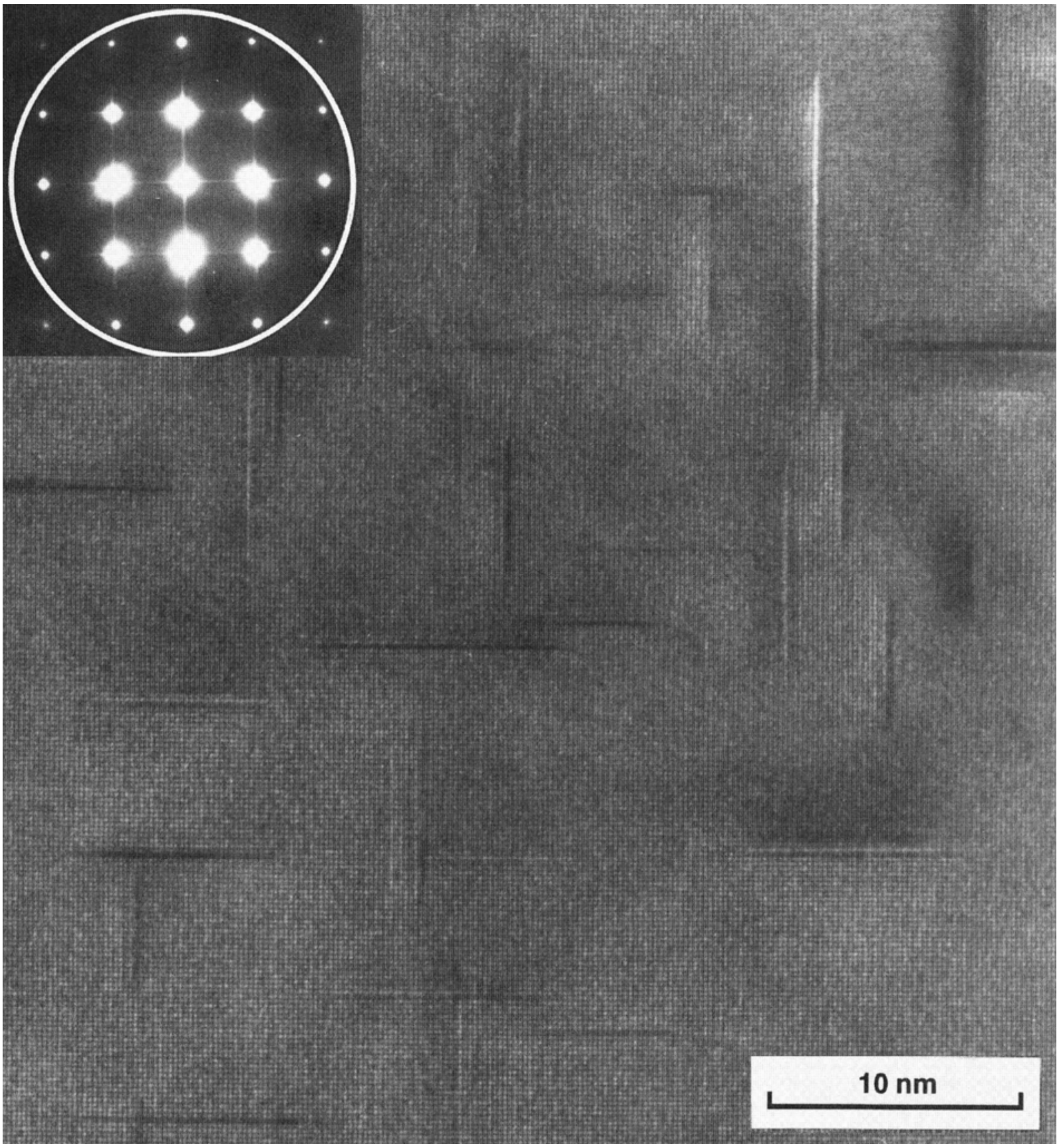

Fig. 1. GP1 zones in the industrial alloy Al–1.68Cu–1.10Mg–0.33Mn at% (2017A) in the T3 temper (pre-strained 2% and naturally aged for more than 2 years); orientation [100], the inset shows the corresponding diffraction pattern, the white circle indicating the contrast aperture position.

If the crystal is tilted 45 degrees around the [010] axis, the atomic columns of [110] direction become parallel to the electron beam. In this orientation, only one set of GP zones remains edge-on. Besides the (200) atomic planes, those of GP zones, two sets of {111} type planes (interplanar spacing of 0.233 nm) are visualised at the same time. In this orientation the contrast is much better as it can be seen in Fig. 2, which presents GP1 zones in Al–1.54at% Cu alloy annealed for 30 h at 100°C.

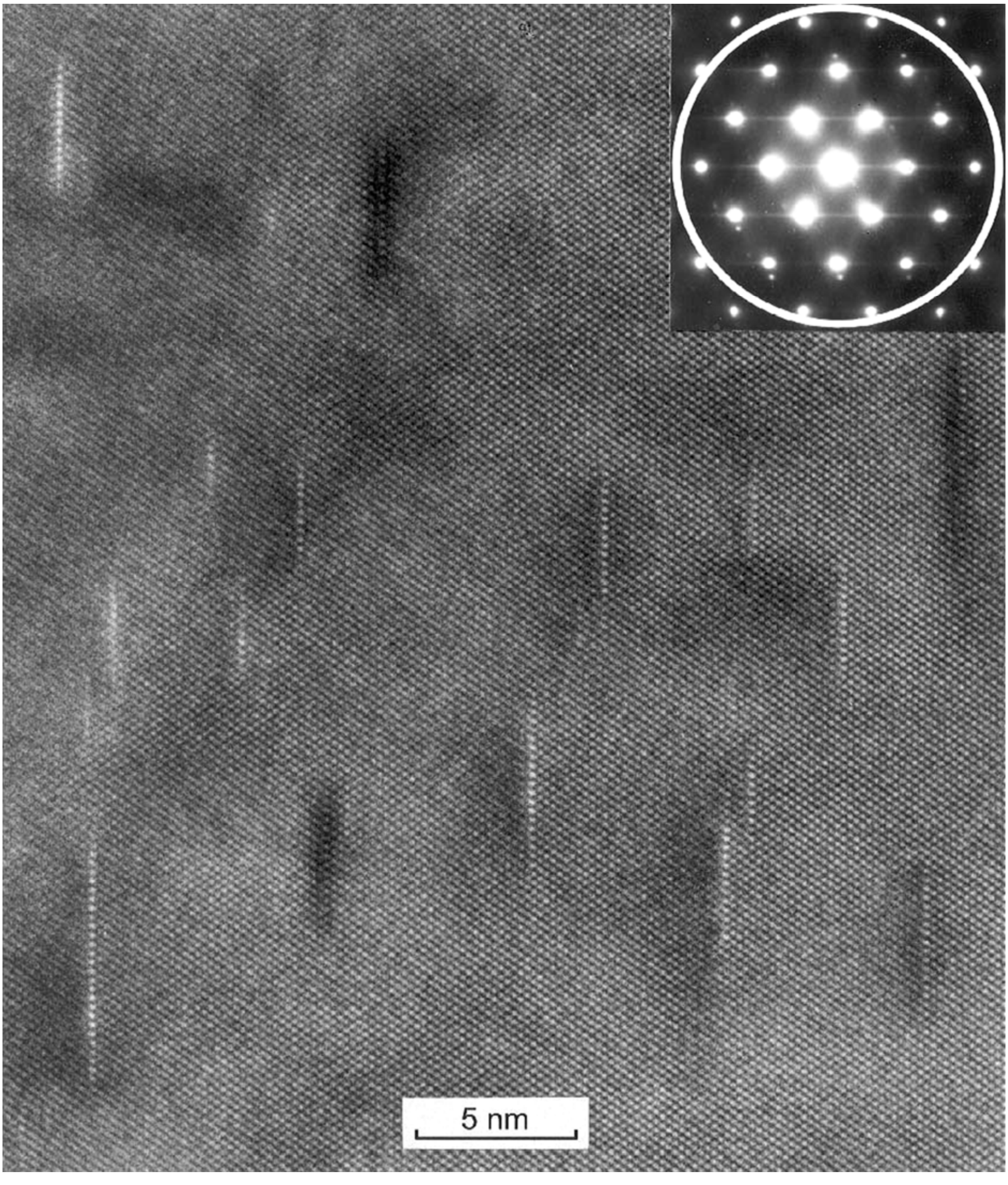

Fig. 2. Monolayer GP1 zones in the Al–1.54at% Cu alloy annealed for 30 h at 100°C; orientation [110]. The inset shows the corresponding diffraction pattern, the white circle indicating the contrast aperture position.

According to simulations, both micrographs represent structure images (at least for the matrix and some GP1 zones), the maxima of interference being situated in the position of atomic columns (in the majority of cases we decided to visualise atoms as white dots). It can be seen that in both crystal orientations the GP1 zones exhibit different types of the contrast. Besides the monolayers, brighter or darker than the matrix columns, more complex structures and types of the contrast can be observed such as a very bright contrast of a monolayer GP zone or very dark ones. If we compare the GP1 zones in the industrial alloy and in the binary alloy, we can conclude that they have the same form - monolayer discs. The difference is only in their size. The GP1 zones in the industrial Al–Cu–Mg–Mn alloy aged more than 2 years at room temperature are in the average somewhat greater than those of the binary Al–Cu alloy annealed 10 h at 100 °C. It could be explained by the presence of Mg and Mn in the industrial alloy (Ando *et al.* [29] observed greater GP zones after the addition of 0.3 % Sn to an Al–2wt% Cu alloy), but the mechanism of growth of the GP zones after alloying by another element is not completely clear.

Even if we can start from the already known models, the explanation of the contrast differences in HREM images of GP1 zones is complicated due to the great number of parameters that influence the formation of the images. The contrast and the image of the GP1 zone change with the foil thickness (unknown *a priori*), the defocus (a relative parameter which can change during the observation due to bending of the foil under the electron beam) and with the size of the GP zone (estimated from its projection). In consequence it is very important to carry out series of simulations.

On the same micrograph GP1 zones appear with contrast which can be extremely different. The simulations calculated in both [100] and [110] crystallographic orientations confirm the experimental observation (Fig. 3) that the contrast is strongly dependent on the defocus. The GP1 zone appears, in many cases of defocus, like a more complex structure than a monolayer. The conditions (defocus - thickness of the foil) to obtain a structure image of the GP1 zone (corresponding to the projected potential) are restricted. There are conditions of defocus, for which the contrast of the GP zone completely disappears. This behaviour renders delicate the work on the statistics of the GP zones which has to be made on the through focus series of the same area. For all these reasons we studied the influence of the different parameters governing the contrast of the GP zones (thickness of the sample, defocusing, size and Cu contents in the GP zones).

Several series of simulations modelling a GP1 zone extending from the top to the bottom of the foils 5 nm, 8.3 nm, 10 nm, 15 nm, 20 nm and 28.3 nm thick respectively enable us to conclude that unless the foil is only 5 nm thick (which is not the case), GP1 zones do not extend through the whole foil thickness, as it was first believed by many investigators. They are located inside the foil or emerge at one of its surfaces.

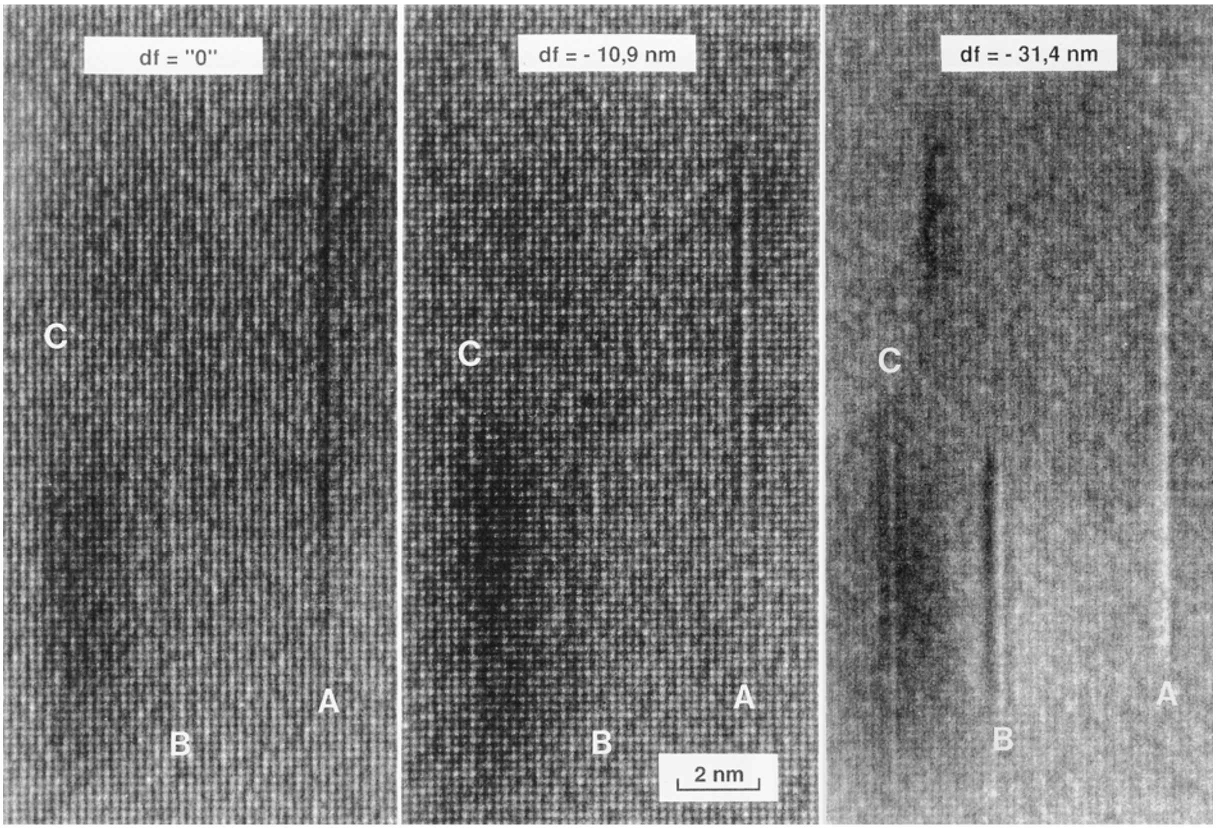

Fig. 3. Variations of contrast of GP1 zones due to the defocus. The GP1 zone A is always visible, while the zone B disappears for the defoci of “0” and –10.9 nm and the GP zone C is invisible for the “0” defocus. Al–1.68Cu–1.10Mg–0.33Mn at% alloy, pre-strained 2% and naturally aged for more than 2 years.

The influence of the foil thickness on the contrast of a GP1 zone is shown in Fig. 4. A GP1 zone of a typical size of 8.3 nm is situated in the middle of the foil. The foil thickness changes gradually from 8.3 nm to 51.2 nm. For each thickness, a series of 14 simulations with defoci ranging from –1 to –79 nm was calculated. Two defoci, –19 and –49 nm, have been chosen to be presented here since they correspond to an experimental through focus series displayed at the same time. From the figure it is obvious that the GP1 zone contrast is very sensitive to the foil thickness. Only two thicknesses (28.3 nm and 51.2 nm) give a change of a complex three-layer contrast to structure image of a monolayer GP zone, like on the micrographs taken in the microscope. The thickness of 28.3 nm has been used as a typical thickness corresponding to the experimental value we obtained from the measurement by electron energy loss spectroscopy (EELS) using plasmon loss.

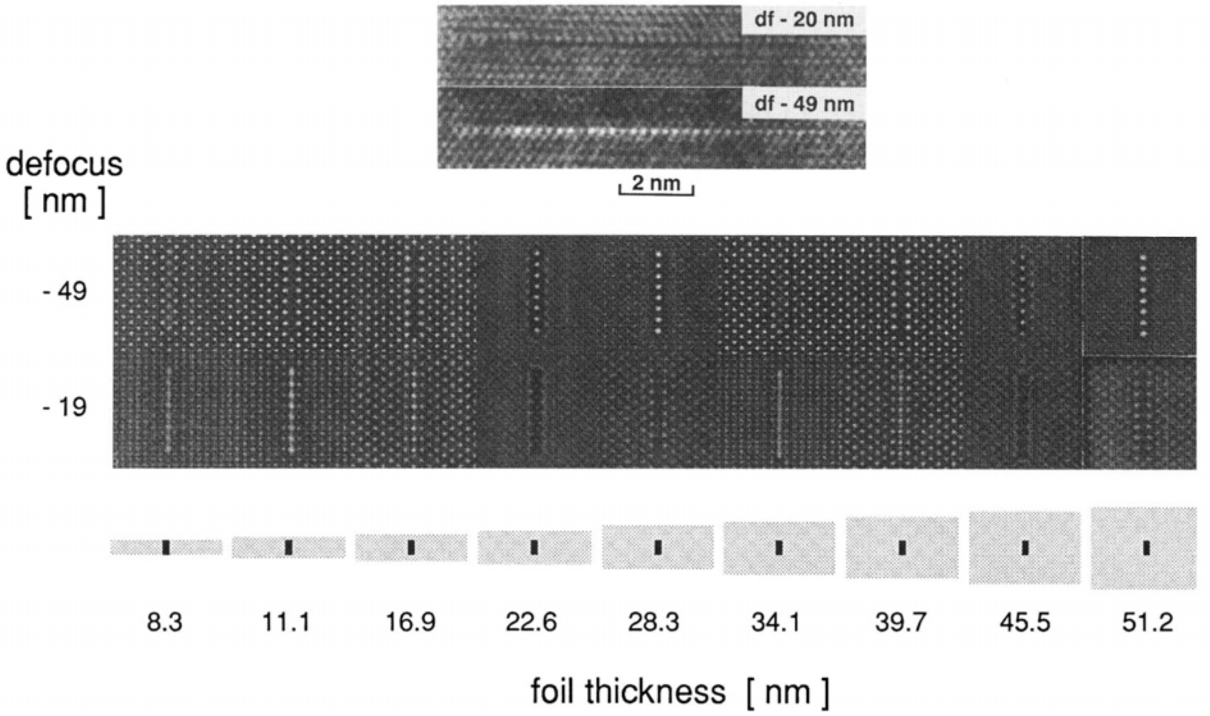

Fig. 4. Simulations of the influence of foil thickness on the contrast of a GP1 zone 8.3 nm in diameter. The variation of the contrast corresponding to experimental images can be found only for two thicknesses, 28.3 nm and 51.2 nm.

As for the position of the GP zone in the "depth" of the foil, the contrast changes are only negligible. Moreover, if we do not take into account surface relaxation, there is no difference, according to simulations, between the contrast of an emerging (truncated) GP zone and that of the GP zone situated close to the surface. The influence of the size of a GP zone (100 % Cu) on the contrast is shown in Fig. 5.

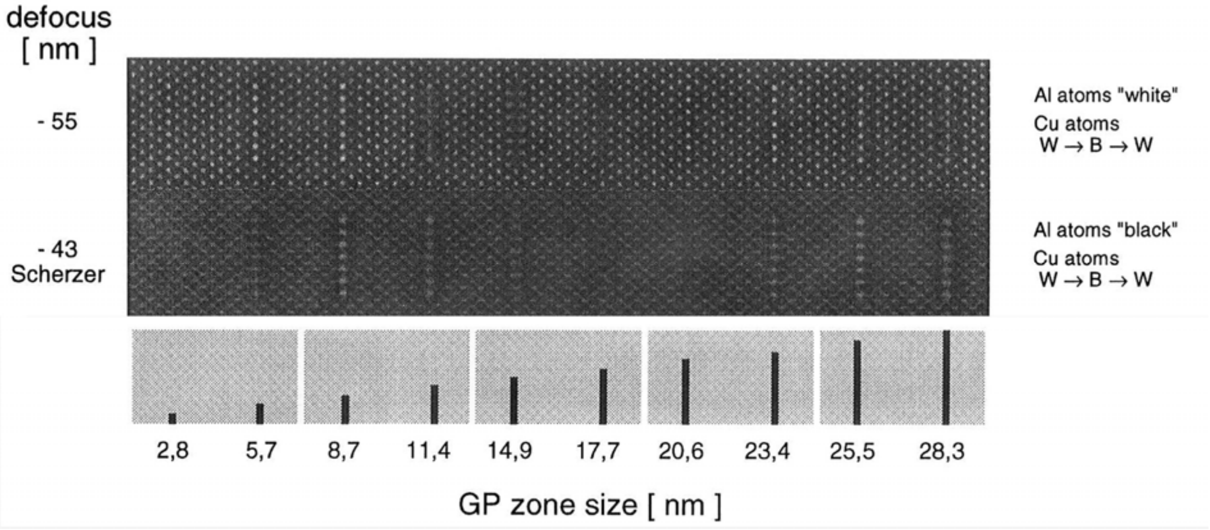

Fig. 5. Influence of the GP1 zone size on the contrast. Series of simulations for GP1 zones composed of 100 % Cu atoms, foil thickness of 28.3 nm.

For a fixed thickness of the foil (28.3 nm), the GP zone size increases gradually from 2.8 nm to 28.3 nm by the step of 2.8 nm (10 atoms of Cu in the column). Four different defoci, –19, –31, –43 and –55 nm respectively, are presented. It is clearly seen, that for a given contrast of the matrix for each defocus, the GP1 zone contrast changes periodically. For instance in the case of the defocus of –55 nm (giving 'white atoms' of the matrix) the Cu columns appear first brighter than the matrix up to the GP zone of 8.7 nm in size, their intensity then decreases (but they appear still as bright dots). For the thickness of 14.9 nm, the Cu rich columns appear dark to reappear bright for the rest of the GP zone sizes. A GP zone 20.6 nm in size has the same contrast as that of only 2.8 nm in size. The periodicity of the contrast is better seen in Fig. 6 presenting a read-out of the intensity of GP zone columns from the simulations of Fig. 5 (defocused –55 nm) in the dependence on the GP zone size and/or on the fraction of Cu atoms in the column. The intensities of one of the centre columns and that of an edge column of this rectangular GP zone are plotted at the same time. The arrow indicates the intensity level of matrix columns. In the majority of cases, the edge GP1 zone columns appear in the simulations brighter than central columns. This contrast reinforcement is due to a change in the interferences of scattered waves by columns of different nature compared to the other columns in the centre of the GP zone. There is an abrupt change of the crystal potential on the edge of a rectangular GP zone used for simulations. In most of the cases the disc shape of the GP1 zones does not permit to observe this contrast experimentally. However, the contrast reinforcement of edge columns has been found on a micrograph of a GP1 zone sheared by a dislocation (Fig. 14).

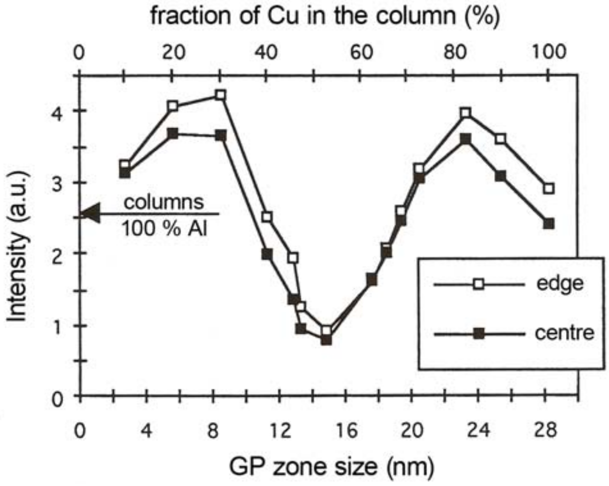

Fig. 6. A read-out of the intensity of GP1 zone columns from the series of simulations of the Fig. 5 defocused –55 nm. The arrow indicates the intensity level of matrix columns.

3.2. Morphology of GP1 zones

In the first models, the GP1 zones were presented as plates or discs. A successive evaporation of atomic layers in the field ion microscope by Abe et al. [6] gave a three dimensional atomic reconstruction of a GP1 zone as an irregular and incomplete plate, containing many clusters of vacancies and ledges.

High resolution electron microscopy gives only a two dimensional projection of the observed structure. However, with the aid of simulations it seems to be possible to obtain supplementary information about the chemical composition and the distribution of atoms in the direction of the projection. Unfortunately, this method is not very sensitive and is very time consuming due to a great number of models to be tested to fit the experimental image. The situation is even more complicated for the interfaces which are not extended through the whole thickness of the thin foil - the case of the majority of our images of GP1 zones. Another complication is the necessity to use the multislice method. If the distribution of atoms in one slice is different to the other, it is necessary to recalculate the projected potential for each slice and the time of the simulation is much increased.

Our observations confirm the results of numerous investigators [5, 10, 12, 13] that the majority of the GP1 zones are monolayers and that more complex structures coexist. However, the GP1 monolayer zones can appear in a variety of contrasts and it is difficult to state in advance whether the difference of the contrast is due to the structure difference or due to the conditions of image formation. Furthermore, as it was already noticed, the statistics are complicated since the contrast depends on the thickness of the foil and the defocus. It is possible to observe, commonly, differences in the contrast of GP1 zones even on the same micrograph. The explanation is the difference in thickness of the foil and/or the tilt of the specimen (if the foil is tilted 15 degrees, the defocus on a same micrograph at the magnification 630k can change for a significant value of 30 nm). Consequently, we are not able to give directly the fraction of the coexisting multilayer GP1 zones. The only possibility to do this correctly by means of HREM is to take many through focus series of GP1 zones, to measure the foil thickness after the exposure of micrographs and to compare the resulting experimental images with the simulations.

We observed, in one of the specimens of the binary Al–1.84 at% Cu alloy aged 10 hours at 100 °C, a localised group of double atomic layer GP1 zones (Fig. 7). This result confirms the observation of the same structure of GP1 zones in the crystal oriented in the [100] direction by Dorignac *et al.* [11]. A through focus series of one of the double layer GP1 zones is in Fig. 8. The contrast changes are important: for the defoci of “0” (being just a reference defocus of our through focus series) and –6.9 nm we observe a very strong contrast, resembling to the contrast of a monolayer. For the next two defoci the contrast decreases until the GP1 zone disappears. The micrograph defocused –35.5 nm represents the structure image. At the defocus of –43.7 nm, the double layer GP1 zone disappears once more and it is again visible if the defocus is –46.4 nm according to the first image (df = "0"). The black area on the left of the GP1 zone can be due to a Bragg reflection on the curved matrix planes (surface relaxation) adjacent to the GP zone which is close to the surface (these black areas are visible frequently on the same side of several GP zones on the micrograph and the effect is stronger for double layer GP1 zones than for the monolayers – see Figs. 2 and 7).

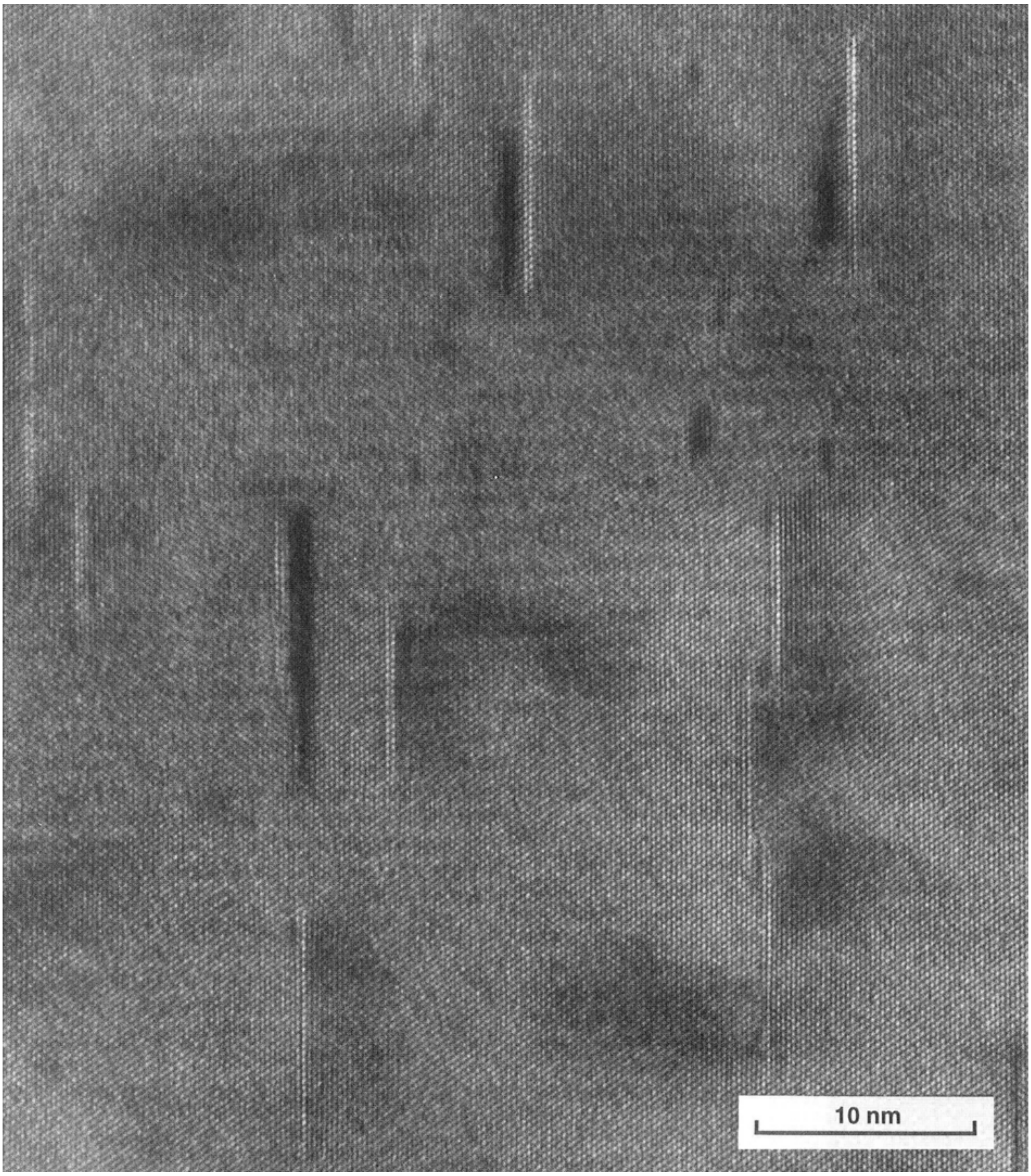

Fig. 7. A group of double layer GP1 zones in the Al–1.84 at% Cu alloy annealed 10 h at 100 °C.

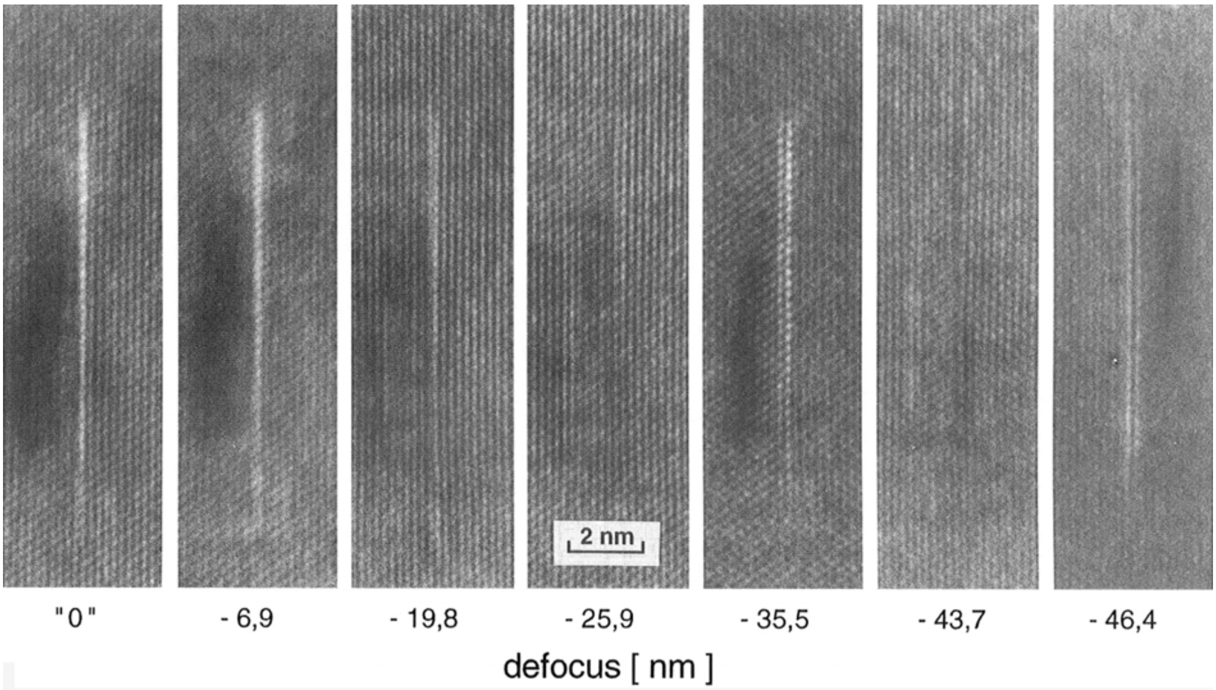

Fig. 8. A through focus series of one of the double layer GP1 zones in Fig. 7. The “0” defocus gives a very strong contrast resembling to the contrast of a monolayer GP zone. The micrograph defocused –35.5 nm represents the structure image.

In the previous paragraph we noticed that, in the simulated images, the edge atomic columns of a rectangular GP1 zone appear somewhat brighter even if they have the same Cu content like central columns of the GP zone. We do not observe this reinforcement of the contrast on the experimental images, since in reality the GP1 zones are disc-shaped and not rectangular. Fig. 9a shows a monolayer, circular shaped GP1 zone showing a decreasing contrast on both its sides. For the small GP1 zones (< 10 nm), a decreasing number of Cu atoms along the GP zone results in a decreasing contrast (Figs. 5, 6). Fig. 9b shows an intensity plot along a simulation of a half-circular GP zone.

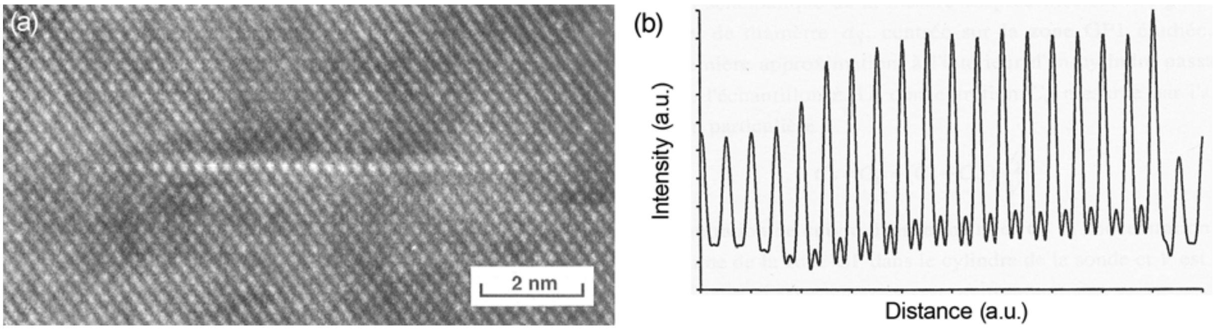

Fig. 9. (a) A monolayer, circular shaped GP1 zone showing a decreasing contrast on both its sides (Al–1.84 at% Cu alloy annealed 10 h at 100 °C); (b) Intensity plot along a simulation of a half-circular GP zone.

In the reality, the discs of GP1 zones are more or less regular, the images like in Fig. 8 being not very common. A decreased intensity (due to greater or smaller number of Cu atoms in the column) in the centre of the projection of the GP1 zone is frequently observed (see Figs. 7,10 and 11).

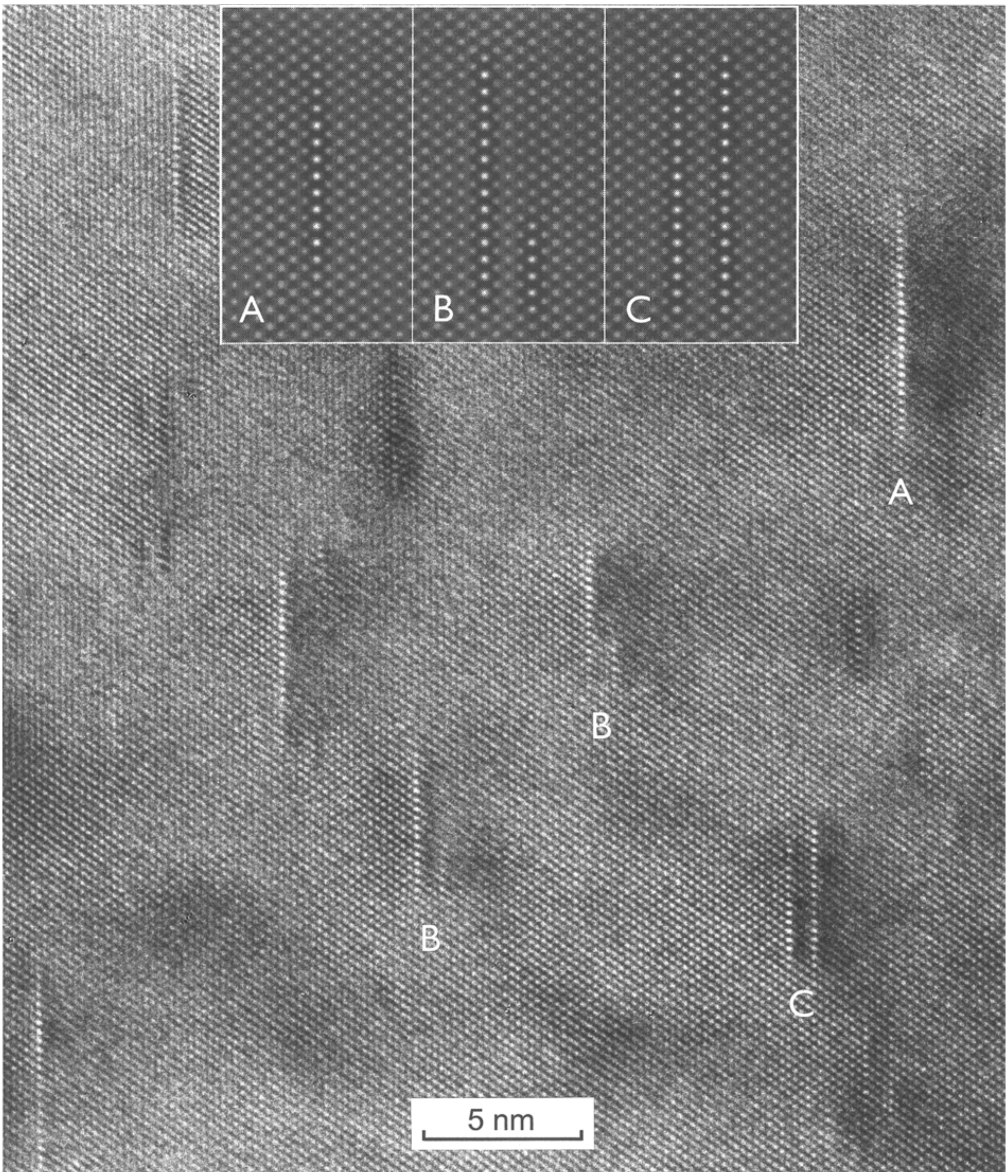

Fig. 10. A group of GP zones having different morphologies: monolayer GP1 zones (A), GP2 zones (C) and particles in an intermediate stage between GP1 and GP2 (B). The inset shows corresponding image simulations for the foil thickness 26.9 nm, GP zones 4.6 nm in size and defocus –55 nm (underfocus with respect to Scherzer defocus –43 nm). Al–1.54 at% Cu alloy annealed 30 h at 100 °C.

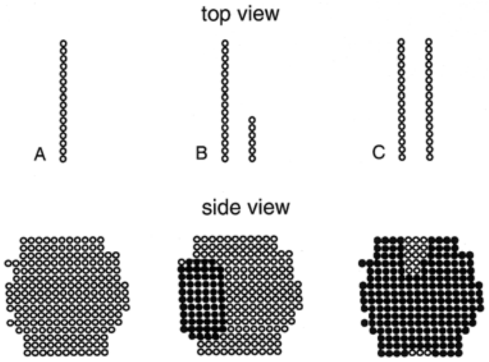

Fig. 11. Models of particles used for the image simulations in Fig. 9.

3.3. Unstable GP zones situated on {111} planes

In the Al–1.84 at% Cu alloy, contrast resembling that of a GP1 zone have been found also on {111} planes (Fig. 12). As can be seen in Fig. 9a, the contrast is almost the same as to that of a regular GP1 zone lying in the {100} type plane, and thus we thing that it is a disc shaped particle rich in copper. The through focus series showed that these GP zones on {111} planes were not stable. Some of them grew under the electron beam, the other being dissolved at the same time. In the literature, these types of contrast in aluminium alloys are frequently interpreted as irradiation defects [30, 31]. On the other hand, Riontino and Zanada [32] observed monolayer and double layer GP zones on {111} planes in a rapidly solidified Al–2 wt% Fe alloy and Yoshida *et al.* [33] report GP zones on {111} planes also in the early period of ageing of Al–3.97 wt% Cu alloy. Our observation can be related to the calculations of Takeda *et al.* [34] suggesting that the difference in the energies between {100} planes and {111} planes is not so important whatever the very large majority of GP zones are in (100) planes. The diffusion of Cu to {111} type planes could be easier due to the formation of point defects under the electron beam. The observation has been made with 200 keV electrons, the energy threshold for the displacement of an Al atom being about 150 keV. However, at 200 keV, the cross section of the interaction is rather small.

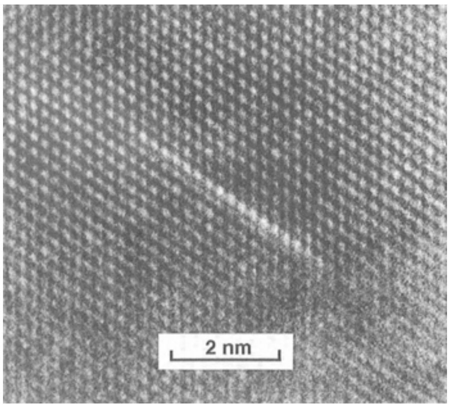

Fig. 12. A GP zone situated on the {111} plane formed during the irradiation by the electron beam, Al–1.84 at% Cu alloy annealed 10 h at 100 °C.

3.4. Determination of Cu content in GP zones using simulations

We used the same model for the GP1 zone containing 100 % Cu and three other models of random distribution of Cu atoms in the GP1 zone (80%, 60% and 40% Cu - balance Al) for the interpretation of a through focus series in Fig. 13.

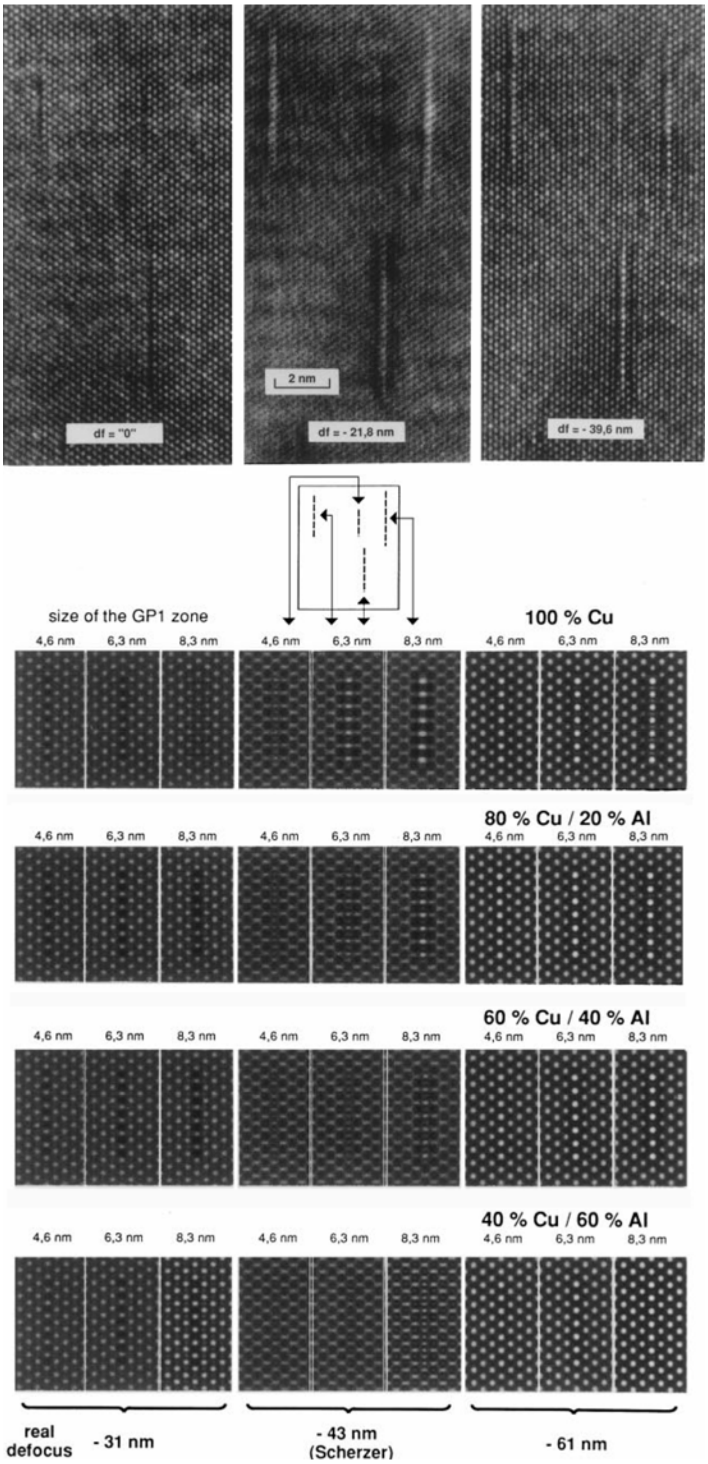

Fig. 13. Interpretation of the contrast changes with the defocus of four GP1 zones having three different sizes (4.6 nm, 6.3 nm and 8.3 nm). Comparison of the experimental images with the simulations calculated for four models of Cu content in the GP1 zone (100 %, 80 %, 60 % and 40 % Cu respectively); Al–1.84 at% Cu alloy annealed 10 h at 100 °C, foil thickness 26.9 nm.

In the micrographs, there are four GP1 zones of three different sizes (4.6 nm, 6.3 nm and 8.3 nm). One of them, 8.3 nm in diameter, disappears completely for the “0” defocus. We simulated the contrast for several foil thicknesses. The best fit has been obtained for 26.9 nm. According to the simulations displayed in Fig. 11 it is obvious that the relative defocus of –21.8 nm (marked on the micrograph) has to correspond in the reality to the Scherzer defocus (–43 nm) since it shows very bright contrast of the GP1 zones on the background of the “black” matrix columns (in the case of aluminium alloys it is not, most of the time, possible to use amorphous matter at the edge of the foil to determine the real defocus as in the case of semiconductors or ceramics). For the relative defocus of –39.6 nm we obtain structure images where the matrix columns are “white” and the Cu rich columns of the GP1 zone too. The distance of these relative defoci is 18.8 nm and thus the real defocus should be –61.8 nm. The simulations for a defocus of –61 nm give, for the 100 % Cu model, a good fit with the experimental image.

On the other hand, the reference defocus (df = “0”) is ”distant” of 21.8 nm from the Scherzer defocus. The real defocus should then be –21.2 nm. However, for this defocus the GP1 zone 8.3 nm in diameter does not disappear for any thickness of the foil. The nearest defocus, for which this GP1 zone disappears, is –31 nm. The difference of 10 nm in the defocus (–31 instead of –21.2 nm) could be explained by the defocus spread of the microscope which is of the same order (and the error on each of the defocus already involved) or by the fact that the foil has changed its "Z" position by bending under the electron beam during the exposure of the through focus series.

Even if we take into account only the defoci of –43 and –61 nm, we can conclude that the copper concentration in all the GP1 zones on the micrograph is 100 % or close to this value. For this concentration we obtain a rather good fit with the experimental images of three sizes of GP1 zones, including the dark fringes adjacent to the GP1 zones (practically inexistent for the GP1 zone 4.6 nm in diameter).

On the other hand, the models containing 40 % Cu / 60 % Al and 60 % Cu / 40 % Al are not in agreement either with the bright contrast of the GP1 zones at the Scherzer defocus, or with the dark fringes adjacent to the GP zones at the defocus of –61 nm. The model of 80 % Cu / 20 % Al is closer to the experimental image than the other two models mentioned above, but the fit for the model of 100 % Cu is clearly the best.

Another experimental image which can be used to estimate the copper content in the GP1 zone from the contrast simulations is shown in Fig. 14. This micrograph was recorded on a specimen, which has been deformed by bending prior to the electrolytic polishing. Consequently many of observed GP1 zones were sheared by dislocations. In Fig. 14, the atomic columns close to the impact of the dislocation appear brighter due to the geometry of the new sheared interface. The edge columns do not have the same neighbours as the other copper rich columns of the GP zone and thus the interferences in the scattering of the incident electron wave are not the same. This effect was first observed on the simulations of rectangular GP1 zones (Figs. 5 and 6). As the real GP zones are disc shaped in most cases (and not rectangular) the contrast fades out with the decreasing number of the copper atoms in the projection (Fig. 9). The only geometry in which we can observe experimentally an abrupt interface (and the reinforcement of the contrast) is this exceptional case of shearing of the GP zone by a dislocation. According to simulations of the sheared rectangular GP zones containing respectively 100 %, 80 %, 60 % and 40 % Cu (shown in the same Fig. 12), the 100% and 80%Cu concentration in the GP1 zone gives the edge columns brighter than the others, which is not so in the case of the models of 60 % and 40 % Cu . Therefore, the copper concentration in this GP zone at least near the sheared edges is in the range of 80 to 100%.

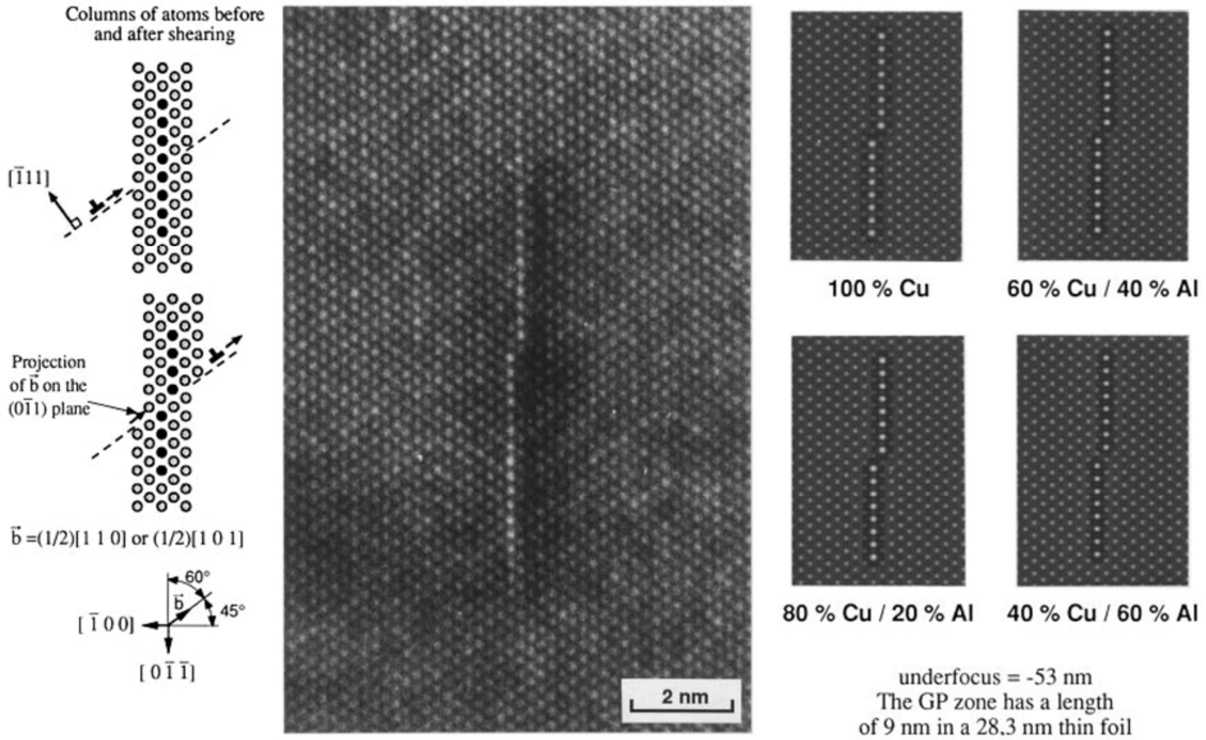

Fig. 14. A monolayer GP1 zone sheared by an edge dislocation. The simulations calculated for four models of Cu content in the rectangular GP1 zone 9 nm in size embedded in the foil 28.3 nm thick are shown at the same time. The reinforcement of the contrast of the edge columns of the impact prove that the image presents really a sheared GP1 zone and not two GP1 zones one close to the other or situated in the different depth of the foil. Furthermore it indicates, according to simulations, that the Cu concentration in the GP zone should be 100 % or close to this value.

3.5. Field Ion Microscopy

GP1 zones parallel to the tip axis

Ion micrographs of single crystal tips, oriented along the <002> axis, present a four-fold symmetry around the (002) pole. The tips are slightly facetted, so the {022} and {024} pole areas are imaged more brightly than the {311} type poles (Fig. 4). The micrograph in Fig. 15 shows a number of GP1 zones with (200) and (020) habit planes that lie parallel to the tip axis (some of them are marked by arrows). This typical contrast is produced by the edges of the GP1 zones arising at the tip surface. This strong contrast is related to the retention of Cu atoms (Al atoms are more easily evaporated). The segments are in fact rows of bright dots, which correspond to individual copper atoms or groups of copper atoms situated on the steps of pole terraces. Atomic resolution is not reached on poles of low Miller indexes, which are the most clearly observed on our FIM micrographs. It is thus difficult to assert if GP1 zones have a monolayer or a double layer structure. Observation of GP1 zones on the top terraces of high Miller index poles was reported by Wada *et al.* [9]. Thanks to the exceptional resolution reached on these particular areas of the FIM image, they identified, in an Al–1.7at% Cu alloy, aged at 130°C for 16h 40min, ten GP1 zones which were all monolayers.

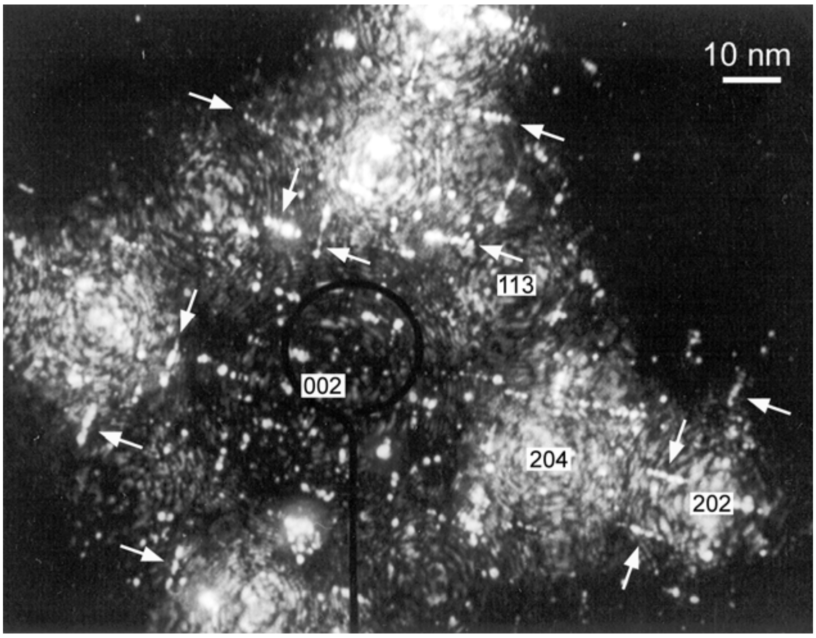

Fig. 15. FIM micrograph of Al-Cu 1.54 at% alloy showing two orientation variants of GP1 zones with their habit planes parallel to the tip axis. The edges of the disc shaped GP1 zones arising at the tip surface are brightly imaged. Some of the monolayers are pointed by arrows.

GP1 zones perpendicular to the tip axis

GP1 zones with their habit plane perpendicular to the tip axis are expected to draw small arcs on all poles of FIM image. But in fact, this variant of GP1 zones was much less frequently detected than the other two and only on the central (002) pole with a multilayer contrast, as illustrated by the micrograph in Fig. 16 – two GP1 zones appearing in a multilayer contrast are pointed out by arrows. This feature was also noticed by Hono *et al.* [8] and can be explained as a preferential retention effect of copper. A slow evaporation of the tip takes place during the FIM observation. In the absence of a GP1 zone, the terraces of the (002) pole shrink regularly as the atoms on the edges evaporate. On the contrary, the copper atoms of a GP1 zone are strongly retained on their terrace edge and prevent the aluminium rich steps which are underneath from evaporating. These Al matrix terraces (covered by a Cu layer) come to protrude as much as the top Cu rich terrace and are thus brightly imaged as well. This produces the multilayer contrast observed on Fig. 5. Fig. 6 displays a schematic representation of the (002) pole terraces, according to the interpretation proposed above. It is impossible to distinguish the one or two copper rich terrace(s) that constitute the GP1 zone from the two or three Al terraces which are underneath and protrude as much as the copper ones. This imaging artefact thus prevents, in this orientation, the determination of the GP1 zone's real thickness and diameter.

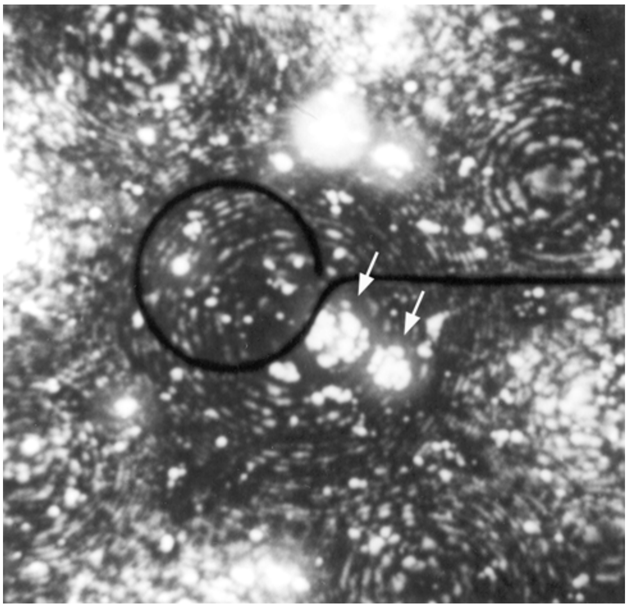

Fig. 16. FIM micrograph of the Al-Cu 1.54 at% alloy. Two GP1 zones with their habit plane perpendicular to the tip axis appear on the (002) pole of the matrix (arrows). The multilayer contrast results from an imaging artefact due to the retention of copper atoms at the tip surface.

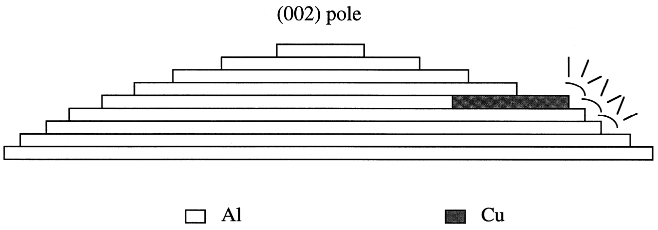

Fig. 17. Schematic cross section of the (002) pole terraces, illustrating the retention effect which produces the multilayer contrast of the GP1 zones with a (002) habit plane shown in Fig. 16. A GP1 zone is a copper rich terrace which prevents the underlying aluminium terraces from evaporating. These aluminium terraces therefore produce the same bright contrasts as the copper rich one and cannot be distinguished from it.

3.5. Tomographic Atom Probe

GP1 zones parallel to the tip axis

TAP analyses were carried out along the axis of the <001>$_{Al}$ oriented tip. GP1 zones with their habit planes parallel to the tip axis are reconstructed as thin, copper rich discs, which are visible on the 3D map of copper distribution in the analysed material. The local copper enrichment is best visible when oriented parallel to the direction of observation, as in Fig. 18.

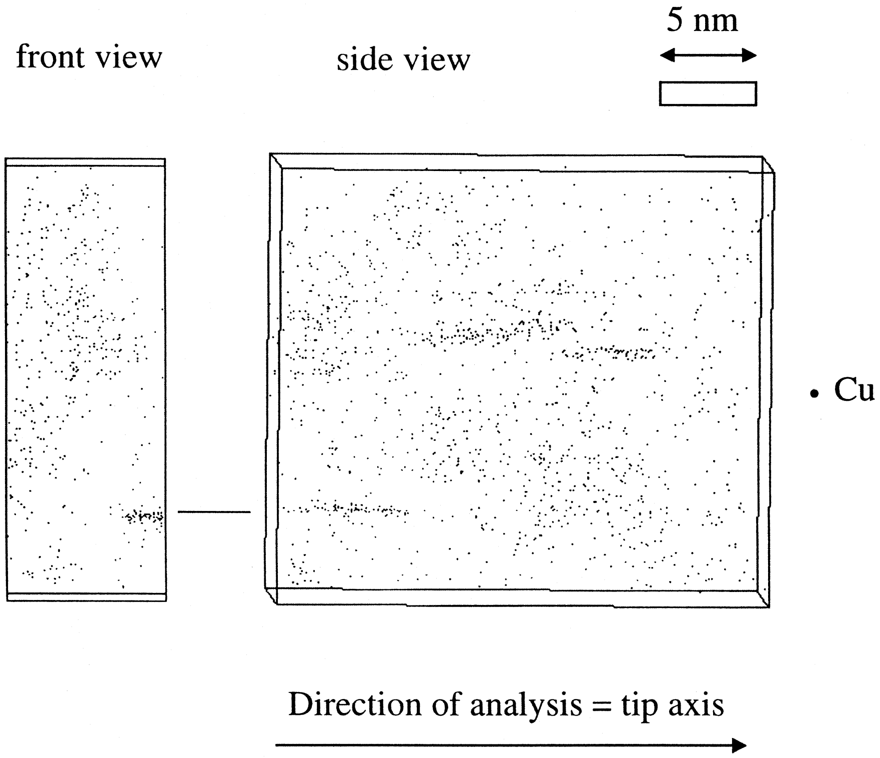

Fig. 18. 3D map of copper atoms in a volume of Al-Cu 1.54 at.% alloy containing GP1 zones parallel to the tip axis. The GP1 zones are reconstructed as thin copper-rich discs, yet thicker than 0.2 nm. This thickness does not reflect the real structure of GP1 zones but results from trajectory aberrations of copper ions lowering locally the resolution of the TAP.

The correct reconstruction of a monolayer platelet requires a lateral resolution better than the spacing of {200} planes, d_{200} = 0.2024 nm, which is not reached in practice. The intrinsic resolution of the TAP detector (< 0.1 nm) is not in question. Ion trajectory aberrations originating from a local magnification phenomenon are responsible for this loss of resolution. Copper atoms are retained at the tip surface and therefore GP zones develop a local radius of curvature higher than that of the aluminium matrix. This behaviour enables the GP zones to be observed by FIM as we discussed above, but also causes the Cu atoms to evaporate with divergent trajectories, which blur the 3D reconstructions.

GP1 zones perpendicular to the tip axis

The retention of Cu atoms at the surface of the tip even more severely disturbs the reconstruction of GP1 zones perpendicular to the tip axis. Whereas the depth resolution of the TAP instrument is sufficient to visualize the stacking of (002) Al planes, GP1 zones do not appear as monolayer Cu rich platelets. The position of a GP1 zone in the analysed volume is revealed by a density modulation in the aluminium map as shown in Fig. 19, and the Cu atoms from the zone are spread and dotty imaged behind it. This is the direct consequence of the evaporation behaviour as it was mentioned in the discussion of the FIM contrast. The resulting TAP reconstruction artefact is further described in [35].

Nevertheless, the 3D reconstructions containing this variant of GP1 zones can provide valuable information. The marks observed in the Al map are disc-shaped. Just as the shape of GP1 zones is reliably restored, the diameter of a mark is thought to reflect that of the corresponding GP1 zone.

Copper content of the GP zones

The composition profile of a GP1 zone is obtained by the following method: a 0.2 nm thick sampling volume is moved step by step throughout the analysed and reconstructed volume of material, in a direction perpendicular to the GP1 zone. Each composition on the profile is calculated from the number of Al and Cu atoms present in the sampling volume at the corresponding level. Convolution with the aluminium matrix is avoided by choosing a sampling volume of smaller size than that of the GP1 zone.

A typical profile through a GP1 zone with a habit plane parallel to the tip axis is represented in Fig. 20. As explained above, reconstructed GP1 zones are thicker than one layer. In the present case, the copper atoms are spread over seven (200) planes and the peak composition reaches 20 at% Cu. The enlargement is not only observed at the centre of the copper rich disc but on its entire surface.

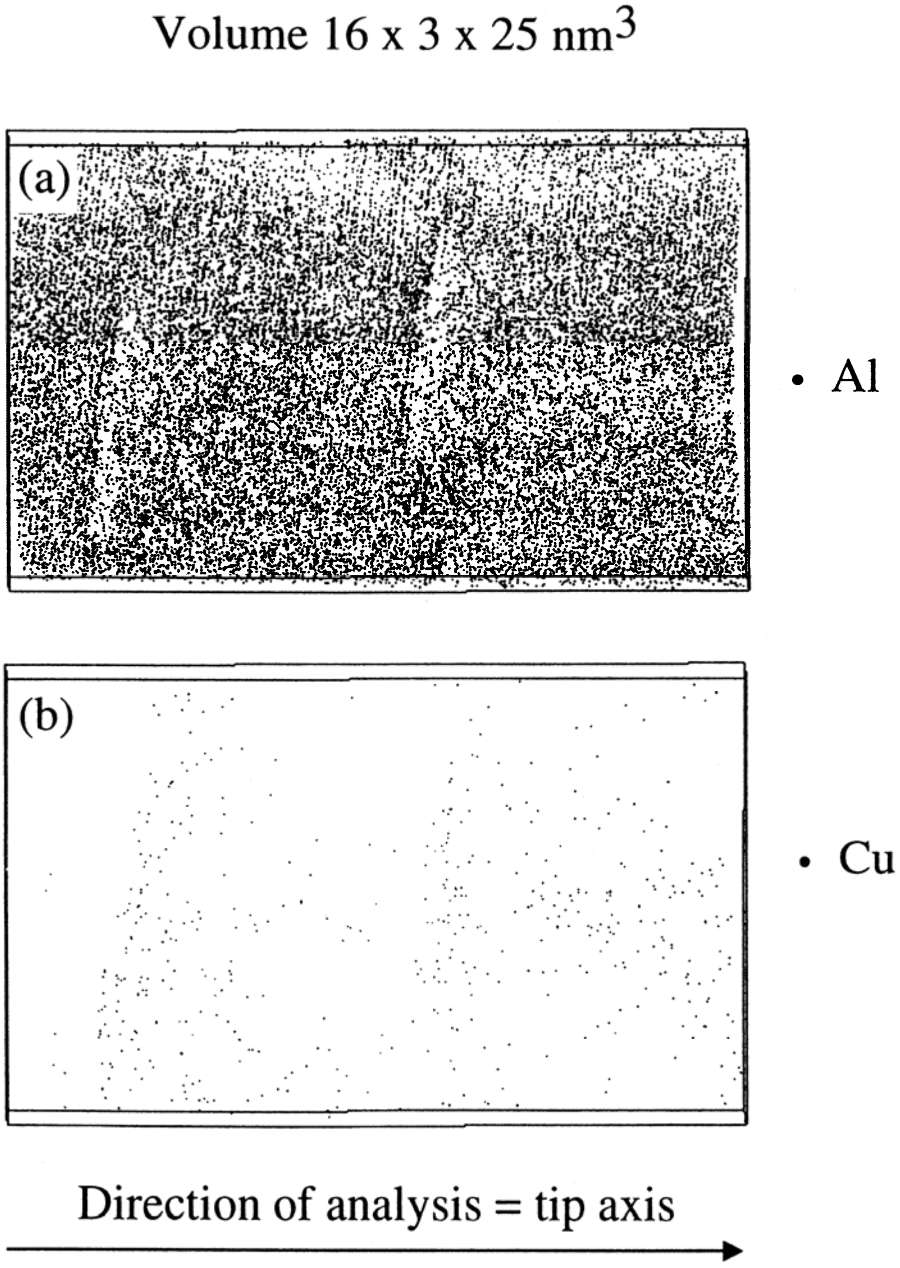

Fig. 19. 3D reconstruction of a volume of Al–1.54 at% Cu alloy containing GP1 zones perpendicular to the tip axis. The position and size of the GP1 zones are revealed by a density change in the aluminium map (a), whereas copper atoms from the zones are spread behind this mark (b). The depth resolution of the TAP enables the (002) plane stacking of aluminium to be reconstructed, but it is locally ruined by GP1 zones' peculiar evaporation behaviour.

This apparent thickness does not reflect the real structure of the GP1 zone. This 3D reconstruction artefact results from the particular evaporation behaviour of copper atoms. Assuming that all the copper atoms collected in the enriched area originate from a single Cu-rich layer in the alloy, the composition of this monolayer GP1 zone is 83 ± 3 at% Cu.

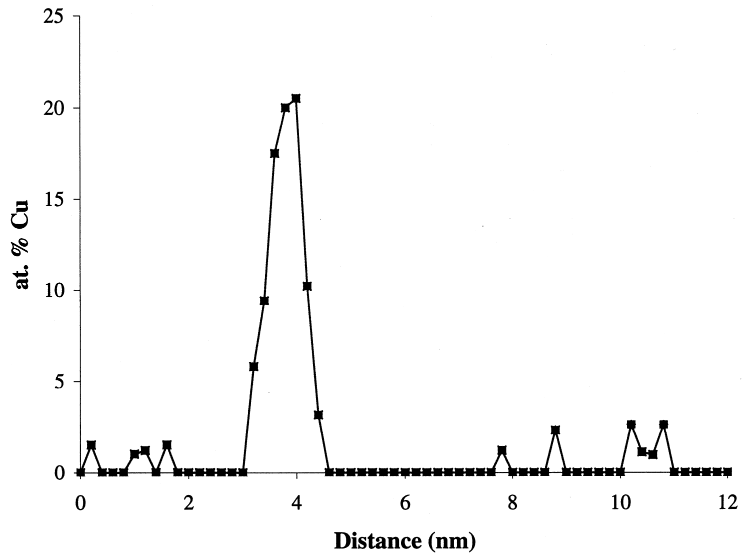

Fig. 20. Copper concentration profile through a GP1 zone with its habit plane parallel to the tip axis. The direction of the profile is perpendicular to the copper-rich disc. The profile reveals the artificial thickness of reconstructed GP1 zones.

The composition profiles of twelve GP1 zones parallel to the tip axis were drawn. The results are given in table 1.

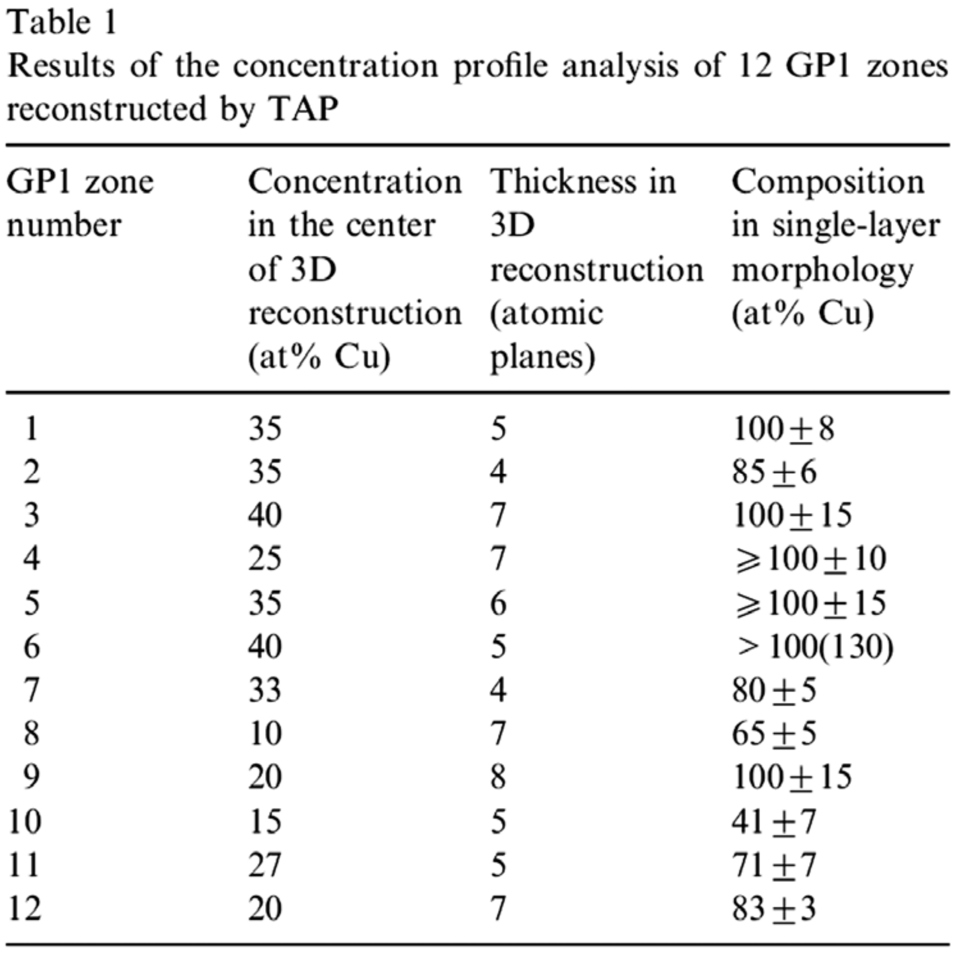

Table 1

Results of the concentration profile analysis of 12 GP1 zones reconstructed by TAP

GP1 zone number	Concentration in the center of 3D reconstruction (at% Cu)	Thickness in 3D reconstruction (atomic planes)	Composition in single-layer morphology (at% Cu)
1	35	5	100±8
2	35	4	85±6
3	40	7	100±15
4	25	7	⩾100±10
5	35	6	⩾100±15
6	40	5	> 100(130)
7	33	4	80±5
8	10	7	65±5
9	20	8	100±15
10	15	5	41±7
11	27	5	71±7
12	20	7	83±3

The thicknesses of these reconstructed GP1 zones range from 4 to 8 layers and their peak compositions from 10 to 40 at% Cu. In the hypothesis of a monolayer structure, three GP1 zones contain 100% Cu. The copper content of three other particles exceeds 100%, when brought to a single atomic layer. These particles could be either double layer GP1 zones as it was observed in Fig. 7 or more probably they are particles in the intermediate state of growth between GP1 and GP2 (θ”) stage as it follows from Fig. 10. Five other GP1 zones contain from 65 ± 5 to 85 ± 5 at% Cu and the composition of the last one is only 41 ± 7 %. It seems therefore that GP1 zones with various copper contents coexist in the alloy.

Copper content of the solid solution

One can notice on 3D reconstructions (Fig.18) that a large amount of copper remains in the solid solution outside of GP1 zones. Direct composition measurements were performed on 3D reconstructed material. Small volumes containing 5 000 to 20 000 atoms were extracted between identified GP1 zones. Their copper contents range from 0.3 ± 0.15 to 1.5 ± 0.2 at% Cu, most of them lying between 0.7 and 1 at% Cu. The fact that both significant as well as negligible depletions in copper are observed in different regions of the aluminium matrix reveals heterogeneity of the copper distribution (there is not an ideal solid solution). From Fig. 20 it is clearly seen that the Cu concentration in the vicinity of the GP1 zones falls down to zero on the distance ranging from 1 to 3 nm (approximately equivalent to 5 to 15 interplanar $(200)_{Al}$ spacings).

4. CONCLUSIONS

It is clear through this study that the contrast analysis of disc shaped GP1 zones in Al–Cu based alloys is extremely complicated. Conclusions on the structure of the GP zones can be correct only after the determination of the foil thickness and of the exact conditions of the image formation. Many different contrasts appear. The conclusion of this work can be summarised as follows:

1) It is confirmed by means of HREM in axial illumination that the majority (> 80 %) of the GP1 zones in Al – 1.84 at% Cu alloy aged at 100 °C for 10 hours are monolayers in the form of discs 4 to 10 nm in diameter. A group of double layer GP1 zones was found in the same alloy aged the same way.

2) GP1 zones in the industrial alloy Al–1.68Cu–1.10Mg–0.33Mn at% (2017A) in the T3 temper (solution annealed at 495 °C, quenched, pre-strained 2% and naturally aged for more than 2 years) have the same form as those observed in the binary alloy. Their diameter is in the average somewhat greater than the diameter of the GP1 zones in the binary alloy.

3) The contrast of the GP1 zones is strongly dependent on their size, on the foil thickness, on the defocus of the objective lens and less sensitive to their internal structure (Cu content) and to the position of the GP zone in the depth of the foil.

4) In the binary Al–1.84 at% Cu alloy, disc shaped monolayer GP zones were found also on {111} type planes. These particles were not stable, some of them have changed their size under the electron beam, and the others disappeared at the same time.

5) HREM and TAP-FIM appear to be complementary techniques for the investigation of GP zones in Al–Cu based alloys. HREM provides the information about the GP zone´s structure and the copper concentration in the GP zones and in the residual solid solution are obtained by TAP.

6) HREM observation of an Al–1.54 at% Cu alloy aged for 30 hours at 100 °C shows that a large majority of the GP1 zones are monolayer discs 1 to 9 nm in diameter. However, some GP2 zones and particles in an intermediate state of growth between GP1 and GP2 stage were also found.

7) TAP results indicate that GP1 zones with different Cu concentration ranging from 40% up to 100% Cu coexist as it was proposed from TEM results. From the total number of twelve GP1 zones examined by TAP, six of them contain 100 % Cu and other five more than 65 % Cu. A GP1 zone with only 40 % Cu was also found.

8) At this stage of the formation of GP1 zones, the copper atoms in the residual solid solution are very heterogeneously distributed. In the vicinity of GP1 particles the Cu content in the matrix falls down to zero, the mean concentration in the solid solution in other regions is between 0.7 and 1 at% Cu.

REFERENCES

[1] GUINIER, A.: Ann. Phys. 12 (1939) 161.

[2] PRESTON, G. D.: Phil. Mag. 26 (1938) 855.

[3] GUINIER, A.: Solid St. Phys. 9 (1959) 293.

[4] AUVRAY, X. – GEORGOPOULOS, P. – COHEN, J.B.: Acta Metall. 29 (1981) 1061.

[5] MATSUBARA, E. – COHEN, J.B.: Acta Metall. 33 (1985) 1945.

[6] ABE, T. – MIYAZAKI, K. – HIRANO, K.-I.: Acta Metall. 30 (1982) 357.

[7] OSAMURA, K. –MURAKAMI, Y. – SATO, T. –TAKAHASHI, T. – ABE, T. – HIRANO, K.-I.: Acta Metall. 31 (1983) 1669.

[8] HONO, K. –SATOH, T. – HIRANO, K.-I.: Phil. Mag. A 53 (1986) 495.

[9] WADA, M. – KITA, H. – MORI, T.: Acta Metall. 33 (1985) 1631.

[10] PHILLIPS, V.A.: Acta Metall. 21 (1973) 219.

[11] DORIGNAC, D. – CASANOVE, M.-J. – JAGUT, R. – JOUFFREY, B.: Electron Microscopy 4 (1980) 174.

[12] SATO, T. – KOJIMA, Y. – TAKAHASHI, T.: Trans. Jap. Inst. Metals 23 (1982) 461.

[13] SATO, T. – TAKAHASHI, T.: Scripta Metall. 22 (1988) 941.

[14] CASANOVE-LAHANA, M.-J. – DORIGNAC, D. – JOUFFREY, B. : In Proc. Inst. Phys. Conf. Ser. No. 61, El. Microsc. and Analysis Group, ed. by M. J. Goringe, IOP Bristol, UK, Vol. 8, 1981, 377.

[15] FONTAINE, A. – LAGARDE, P. – NAUDON, A. – RAOUX, D. – SPANJAARD, D. : Phil. Mag. B 40 (1979) 17.

[16] WOLVERTON, C.: Phil. Mag. Lett. 79 (1999) 691.

[17] GEROLD, V. – BUBECK, E.: Scripta Metall. 22 (1988) 953.

[18] HONO, K. – HASHIZUME, T. – HASEGAWA, Y. – HIRANO, K. – SAKURAI, T.: Scripta Metall. 20 (1986) 487.

[19] MALIK, A. – SCHÖNFELD, B. – KOSTORZ, G. – BÜHRER, W. – PEDERSEN, J.S.: Z. Metallkd. 88 (1997) 8.

[20] GEROLD, V.: Scripta Metall. 22 (1988) 927.

[21] SCHÖNFELD, B.: Progress Mater. Sci. 44 (1999) 435.

[22] RINGER, S.P. – HONO, K.: Mater. Charact. 44 (2000) 101.

[23] KONNO, T.J. – KAWASAKI, M. – HIRAGA, K. Phil. Mag. B 81 (2001) 1713.

[24] BLAVETTE, D. – DECONIHOUT, B. – BOSTEL, A. – SARRAU, J. – MENAND, A.: Rev. Sci. Instr. 64 (1993), 2911.

[25] KARLÍK, M. – JOUFFREY, B.: Acta Mater. 45 (1997) 3251.

[26] KARLÍK, M. – JOUFFREY, B. – BELLIOT, S.: Acta Mater. 46 (1998) 1817.

[27] KARLÍK, M. – BIGOT, A. – JOUFFREY, B. – AUGER, P. – BELLIOT, S.: Ultramicroscopy, 98 (2004) 219.

[28] STADELMANN, P. :, Ultramicroscopy 21 (1987) 131-146.

[29] ANDO, Y. – MIHAMA, K. – TAKAHASHI T. – KOJIMA, Y.: Acta Metall. A31 (1975) S263.

[30] ALFONSO, C. – CHARAI, A. – ZAHRA, C.Y. – ZAHRA A.M.: in Proc. 13th Int. Cong. El. Microsc., ed. by B. Jouffrey et al., Les Editions de Physique, Paris, Vol. 2A, 1994, 689.

[31] MINGLER, B. – KARNTHALER, H. P.: ibid, p. 103.

[32] RIONTINO, G. – ZANADA, A.: ibid. p. 443.

[33] YOSHIDA, H. – HASHIMOTO, H. – YOKOTA, Y. – AJIKA, N.: Trans. Jap. Inst. Metals 24 (1983) 378.

[34] TAKEDA, M. – OKA, H. – ONAKA, I.: Phys. Stat. Sol. (a), 132 (1992) 305.

[35] BIGOT, A. – DANOIX, F. – AUGER, P. – BLAVETTE, D. – MENAND, A.: Appl. Surf. Sci. 94/95 (1996) 261.

CURRICULUM VITAE

Doc. Dr. RNDr. Miroslav KARLÍK

EDUCATION AND PROFESSIONAL CAREER

1979–1984	Charles University, Prague, Solid State Physics (MSc.)
1984–1991	Research Institute for Metals, Panenské Břežany, Researcher
1986	Charles University, Prague, Solid State Physics (RNDr.)
1991–1994	École Centrale Paris, France, doctoral thesis (Dr.)
1995–2003	Czech Technical University in Prague, Faculty of Nuclear Sciences and Physical Engineering, Department of Materials, Assistant Professor
2003– present	Czech Technical University in Prague, Faculty of Nuclear Sciences and Physical Engineering, Department of Materials, Associate Professor, Physical and Materials Engineering (Doc.)

TEACHING EXPERIENCE

1991–1994	École Centrale Paris (Practical of Physics)
1995– present	Charles University (High Resolution Electron Microscopy)
	Czech Technical University in Prague (Metal Physics 2, Physical Metallurgy 1, Non-metallic Materials, Materials Science)
	Supervising and guiding bachelor's and master's degree projects and PhD theses.

RESEARCH INTERESTS

Microstructure and mechanical properties of materials: physical metallurgy and processing of Al alloys, properties of steels and intermetallics based on Fe_3Al and FeAl, transmission electron microscopy.

PUBLICATIONS

Author or co-author of 54 papers in journals, 89 contributions in conference proceedings and 29 research reports for Czech and foreign customers. The papers recorded more than 190 citations (over 130 in the ISI Web of Science database).

RESEARCH GRANTS AWARDED

EUREKA 1824 FINSTOCKS, (1998–2001), Development of aluminium alloy sheet with improved plasticity for finstock application

Czech-French project BARRANDE (2001–05–01, 2001–2002), Influence of the distribution of the second phase particles on the fracture toughness of low-alloy steel (prof. Bompard, École Centrale Paris)

EUREKA 2530 CONTCASTCALTRANS, (2001–2004), Continuous casting technologies for production of aluminium alloy sheets for transportation applications

Czech Science Foundation (GAČR 106/02/0687, 2002–2004) Modification of the properties of intermetallic alloys based on Fe_3Al by thermo-mechanical treatment and additives

Ministry of Education, Youth and Sports (MŠMT – 1K03001, 2003–2005) Mechanisms of the ductile-to-brittle transition in steels

Czech Science Foundation (GAČR 106/04/0066, 2004–2006), Physical aspects of the transition behaviour of ferritic steels

RESEARCH FELLOWSHIPS

Laboratoire de Mécanique, Sols, Structures et Matériaux, École Centrale Paris, France, Prof. Bernard Jouffrey, 2 months in 1996

Department of Materials Science and Engineering, Kyoto University, Japan, Prof. Masaharu Yamaguchi, 3 months in 1997

Laboratoire de Mécanique, Sols, Structures et Matériaux, École Centrale Paris, France, Prof. Philippe Bompard, 13 months in the period 2001–2007

MEMBERSHIPS

Metals Science Society

Czechoslovak Microscopy Society

RESERCH AND EDUCATION - FUTURE PROSPECTS

In the following two years the research activities of the Department of Materials of the Faculty of Nuclear Sciences and Physical Engineering, Czech Technical University in Prague, will continue as part of two long-term research projects supported by the Ministry Education, Youth, and Sports of the Czech Republic: MSM6840770021 “Diagnostics of materials” and MSM6840770020 “Safety of nuclear facilities”. Simultaneously, several new application projects are under way in cooperation with various industrial partners. For example, my research group cooperates with the Czech producer of Al sheets, AL INVEST Břidličná, on the development of recrystallization-resistant Al-Mn thin foils for soldered car heat exchangers. The experience acquired in our department during the previous research of Al alloys thus can be applied to the processing technology at industrial scale.

On the completion of all the above-mentioned projects, we intend to submit new research project proposals to the Czech Science Foundation (GA ČR), Czech Technology Foundation (TA ČR), or CTU Science Foundation. Two topics of the proposals will cover optimization of the properties of Fe-Al based intermetallics and plasma-sprayed coatings from this promising material. I would also like to continue the research of Al-based alloys. In this field, my attention has concentrated on improving the properties of the recently developed Al-Cu alloy with tin addition fabricated in the form of extrusions by ALCAN Děčín. This material has a potential to replace lead-containing machinable alloys and to contribute to the amelioration of the environment. Furthermore, the former international cooperation of our department with ALCAN Research Centre in Voreppe, France could thus be restored.

The education in materials science in our department, set up since its foundation in 1962, has an interdisciplinary character. The students are given a deep knowledge of physics of materials on the one hand, and applied mechanics and failure analysis on the other hand. Besides the classical lectures, exercises, seminars and practicals, the students are involved in a system of individual research projects linked to the main research interests of the department. My contribution to this highly successful concept is to provide the students with the best knowledge of physical metallurgy and non-metallic materials through my lectures and to supervise the bachelor’s, and master’s degree projects, and PhD theses.

Being a specialist in transmission electron microscopy (TEM), I have written a textbook covering the basics as well as recent advances in this important field of materials characterization. I plan to introduce a new optional lecture for the 2nd year students in order to extend their knowledge about the possibilities of the study of the structure and local chemical composition of condensed matter. At present, TEM has a routinely attainable atomic scale resolution, making it very important especially in the nanometric approach.